Ann. Rev. Fluid Mech. 1979. 11: 371–400

ON THE SPREADING OF LIQUIDS ON SOLID SURFACES: STATIC AND DYNAMIC CONTACT LINES

*8146

E. B. Dussan V.
Department of Chemical and Biochemical Engineering, University of Pennsylvania, Philadelphia, Pennsylvania 19104

INTRODUCTION

A contact line is formed at the intersection of two immiscible fluids and a solid. That the mutual interaction between the three materials in the immediate vicinity of a contact line can significantly affect the statics as well as the dynamics of an entire flow field is demonstrated by the behavior of two immiscible fluids in a capillary. It is well known that the height to which a column of liquid will rise in a vertical circular capillary with small radius, a, whose lower end is placed into a bath, is given by $(2\sigma/a\rho g)\cos\theta$, where σ is the surface tension of the air/liquid interface, θ is the static contact angle as measured from the liquid side of the contact line, ρ is the density, and g is the magnitude of the acceleration due to gravity.[1] Thus, depending on the value of the contact angle, θ, which is a direct consequence of the molecular interactions among the three materials at the contact line, the height can take on any value within the interval $[-2\sigma/a\rho g, 2\sigma/a\rho g]$. In a sense, the influence of the contact angle is indirect: the contact angle, in capillaries with small radii, controls the radius of curvature of the meniscus which, in turn, regulates the pressure in the liquid under the meniscus. It is this pressure that determines the height of the column.

In a similar manner, the *dynamic* contact angle can influence the *rate* of displacement of the meniscus through the capillary. The pressure drop

[1] If the radius is not small then the height can be determined by using the results of Concus (1968).

0066-4189/79/0115-0371$01.00

that must be imposed between the air in front of the meniscus and the liquid at a distance L behind the meniscus in order to produce a given volumetric flow rate, Q, is given by $8Q\mu L/\pi a^4 - (2\sigma/a)\cos\theta$, where μ is the viscosity of the liquid. This formulation, due to West (1912), although it is often attributed to Washburn (1921), represents the first successful analysis of a system with a moving contact line. If $(2\sigma/a)\cos\theta$ is comparable in size to $8Q\mu L/\pi a^4$, then the dynamic contact angle is important. Insofar as the contact angle depends on the speed of the contact line, $Q/\pi a^2$, the dynamics of the fluids in the immediate vicinity of the moving contact line cannot be ignored.

THE STATIC CONTACT ANGLE

Young (1805) was the first person to derive an expression for the static contact angle, θ_S. Upon assuming that the three material boundaries—gas/liquid, liquid/solid, and solid/gas—each possess a constant surface *tension*, he reasoned that in order for the system to be in static equilibrium, their horizontal components must sum to zero at the contact line (refer to Figure 1). This condition

$$\sigma_{LG}\cos\theta_S = \sigma_{GS} - \sigma_{LS} \tag{1}$$

is often referred to as Young's equation. Deceiving in its simplicity, this equation has eluded experimental verification due to an inability to measure σ_{GS} and σ_{LS}. Reported "measured values" of $\sigma_{GS} - \sigma_{LS}$ are often obtained by substituting measured values of σ_{LS} and θ_S into Equation (1).

The above derivation is not totally satisfying from a mechanical point of view. Static equilibrium requires *all* of the forces to be balanced. In order to balance the vertical component of the surface-tension forces at the contact line, one must admit to the existence of a reaction force in

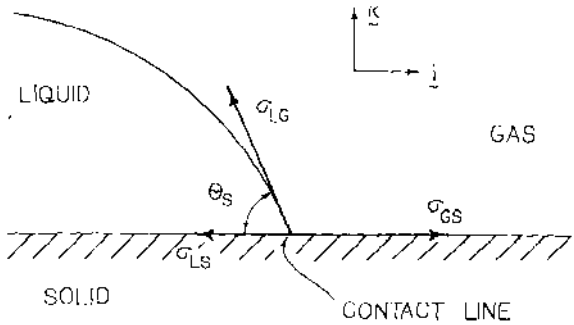

Figure 1 The configuration of three materials—gas, liquid, and solid—in static equilibrium.

the solid, $-\mathbf{k}\sigma_{LG} \sin \theta_S$. That this force *can* exist is not in question, since the solid is being implicitly modeled as a rigid body. What restricts this force to having only a vertical component? If, in addition, a horizontal component were allowed, then all forces acting at the contact line could be balanced for *any* value of the contact angle!

On the other hand, a system is in static equilibrium if it is in a configuration of minimum energy (Gibbs 1906). The appearance of surface tension in the equation of conservation of linear momentum necessitates the inclusion of an expression for surface *energy* in the equation of conservation of energy. Gauss (1829) has shown that Equation (1) is exactly the end-point condition in the associated variational problem. A demonstration appears in Gibbs (on p. 326) along with an excellent discussion on the nature of interfaces (pp. 219–349). While Gauss has provided a rigorous theoretical basis for Equation (1)—a direct consequence of which is that the static contact angle is a *unique* property of the materials—this usually disagrees with experimental observations.

Various techniques have been used to measure the contact angle. One popular method consists of placing a drop of liquid on a flat horizontal surface. It can be deposited by an external device located above the surface, or it can be formed by forcing liquid through a small hole in the surface. The contact angle can be measured, either directly by drawing on an enlarged photograph a line tangent to the gas/liquid interface at the contact line and using a protractor, or indirectly by using the solution for the shape of the meniscus (Padday 1969) along with the measured height of the apex of the drop and its volume. Instead of a drop, similar procedures may be employed with a partially submerged vertical flat plate. The contact angle can be determined, either directly from a photograph, or indirectly by measuring the vertical position of the contact line with respect to the undisturbed level of the liquid, along with the solution for the shape
contact angle can also be determined by measuring the force necessary to keep the plate partially submerged in the liquid at a known depth, along with a simple calculation of the force balance. Another technique consists of measuring the angle at which the plate must be "tilted" with respect to the vertical so that the liquid/gas interface appears horizontal all the way up to the contact line. All these methods have varying degrees of accuracy. Some have a reported accuracy of $\pm 0.1°$; however, the limiting factor usually lies in the reproducibility of the measurements. It is rare for contact angles to be reported with less uncertainty than $\pm 1.0°$ to $2.0°$.

It is important to realize that even though static contact angles are reported, the most careful experimenters deduce its value from *dynamic*

measurements. We will consider the contact line illustrated in Figure 1 to be advancing when its velocity, $U\mathbf{i}$, is positive, i.e. $U > 0$; the contact angle, θ, is calculated from the liquid side of the contact line as is done with θ_S. Typical experimental results appear in Figure 2. It is always found that $\partial\theta/\partial U \geqq 0$ whether or not the other fluid is a gas or an immiscible liquid. The extrapolated value of θ in the limit as $U \to 0$ with $U > 0$ ($U < 0$) is called the *advancing* (receding) contact angle, θ_A (θ_R). The magnitude of the smallest reported speed, U_C, can be due to limitations in the equipment, or it can indicate the speed at which a transition occurs: at speeds greater than U_C, the contact line movement is very smooth; and, at speeds less the U_C, the motion of the contact line appears to be unsteady and spasmatic (often referred to as "stick slip"). As evidence of the latter, Blake (1968) was able to reduce U_C from about 0.03 cm sec^{-1} for a system consisting of benzene-water-Pyrex borosilicate glass, to about 0.03×10^{-2} cm sec^{-1} by pretreating the glass with dimethyldichlorosilane (the same apparatus was used in both cases). In any given experiment, it is not at all obvious how slow is "slow" for the purpose of accurately extrapolating values of θ_A (θ_R); e.g. Blake found that the contact angle decreased in value by about 10° as the speed of the contact line decreased from 0.03 cm sec^{-1} to 0.03×10^{-2} cm sec^{-1} in his system consisting of pretreated glass. However, it is rare for results to be reported for speeds less than a few micrometers per second. Occasionally one finds two data points reported exactly at $U = 0$, denoted by θ'_A and θ'_R

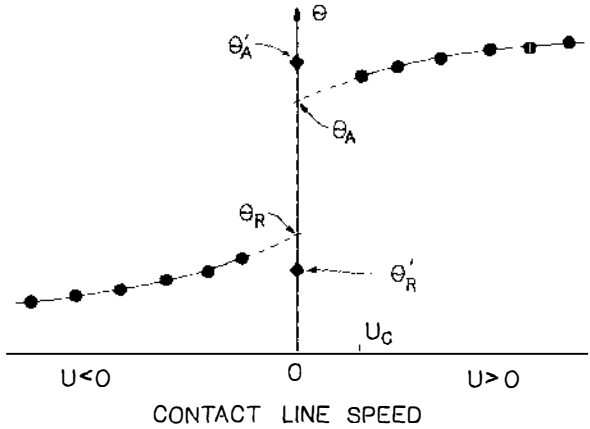

Figure 2 Typical experimental results for the dependence of the dynamic contact angle, θ, on the speed of the contact line. When $U > 0$ ($U < 0$) the contact line is advancing (receding). U_c denotes the slowest speed at which an experimental measurement is made.

in Figure 2. These angles are usually measured with a different experimental apparatus (Elliott & Riddiford 1967) in which the contact line is initially static and the contact angle is varied until the contact line is observed to move. It is not at all obvious whether or not a difference in measured values between θ'_A and θ_A, or θ'_R and θ_R, is real or due to experimental error. In any case, there is no question that for many material systems there exists an interval $[\theta_R, \theta_A]$, with the property that if θ lies within this interval then the contact line does not appear to move. This nonuniqueness in the static contact angle is often referred to as *contact-angle hysteresis.*

Even though contact angle hysteresis seems to be the rule, material systems have been reported in which the static contact angle is unique. Upon submerging a smooth clean solid surface (being "mirror" smooth seems to be important) into a bath of polar solute and nonpolar solvent, such as heptadecylamine in white mineral oil, the character of the surface of the solid is completely changed. A monolayer (short for monomolecular-layer) of the polar solute adsorbs onto the solid, and remains there even after it is removed from the bath. Zisman (1964) has examined extensively the contact angles formed by many different liquids placed on a wide variety of solid surfaces prepared in this way, referred to as the *retraction method.* He finds that on surfaces with adsorbed organic monolayers, it is unusual for the advancing and receding contact angle to be different provided that water is not used. Apparently the nature of the surface is so completely determined by the adsorbed molecules in the monolayer that the static contact angle does not change even if a different solid is used or if adsorption takes place in a different solvent.

Since it is usual for more than one contact angle to be observed it is evident that the model proposed by Young and Gauss—that material boundaries have a constant surface tension (or energy)—is insufficient. Numerous attempts have been made in the last 25 years to identify its deficiencies. One often-criticized assumption is that the solid surface remains undeformed at the contact line. This is nurtured by the fact that a concentrated load applied along a line on the surface of a linearly elastic solid gives rise to a singular solution in the neighborhood of the line, i.e. the displacement vector becomes unbounded as the line is approached from within the solid. Lester (1961), by allowing the fluid-fluid interface to have a finite thickness [he assumed it to be 10 Å, a reasonable estimate in light of more current studies (Chapela et al 1977)], throughout which the surface tension was assumed to be uniformly distributed, has shown quite convincingly that for ordinary solids—glass and metal as opposed to gels—the deformation near the contact line is

very small and negligible.[2] Hence, modeling the solid as rigid and the fluid-fluid interface as a surface having no thickness is perfectly acceptable from this point of view.

An experimentally verified cause of contact-angle hysteresis is roughness of the surface of the solid. Only by coating very smooth surfaces could Zisman achieve $\theta_A = \theta_R$. To illustrate its potential effect from an analytic point of view, Johnson & Dettre (1964) examine the static configuration of an axially symmetric drop of liquid placed on a "highly idealized" model of a rough surface. The solid surface, though appearing to be horizontal and flat when viewed from a length scale that characterizes the size of the drop, has concentric axially symmetric scratches in the form of the sine wave. Under these conditions the *observed* contact angle, θ, can differ quite a bit from the *actual* contact angle, θ_S; refer to configuration A in Figure 3. However, more than one static configuration is possible as indicated by B in Figure 3. Thus, the observed contact angle, θ, is not unique even though only one value of θ_S has been assumed. In addition, it can be shown that all possible observed angles lie within a bounded calculable interval. This is very suggestive of contact-angle hysteresis, which is characterized by the interval $[\theta_R, \theta_A]$, despite the fact that for this particular example only a finite number of distinct angles within the interval correspond to possible static configurations. Needless to say, one would never expect a surface to have such an idealized form; also, non-axially symmetric shapes must be taken into account. Huh & Mason (1977) take a step in this direction by analyzing non-axially symmetric shapes of drops on surfaces of solids with cross, hexagonal, concentric, and radial grooves, as well as one that is supposed to typify random roughness. They use a perturbation method that restricts them to shapes of drops closely resembling spherical caps. Even though they admit to weaknesses in their solutions,[3] they report two average characteristics of the surface upon which the observable contact angle depends: the ratio between the actual and apparent area of contact between the solid and the liquid, and a "surface texture factor." In general, there is no question that surface roughness significantly affects contact-angle hysteresis; however, for "real" surfaces it has defied prediction. There is one known basic "rule of thumb": θ_A will decrease (increase) in value by roughening a surface for which $\theta_A < 90°$ ($> 90°$).

[2] The analysis has some shortcomings: it is only correct for a contact angle of 90°; and the use of Neumann's triangle is ad hoc.

[3] The two more serious weaknesses seem to be the lack of complete agreement between the perturbation and exact solution for the case analyzed by Johnson & Dettre; and an inability to predict more than one shape for a drop of a given volume. It is the latter that prevents them from predicting contact-angle hysteresis.

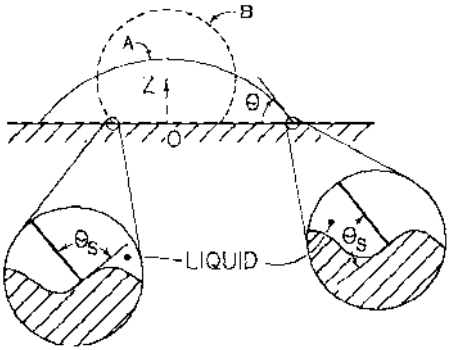

Figure 3 The surface of the solid has a sine-wave corrugation, as seen in the two magnified views, and has rotational symmetry about the Z axis. A finite number of static configurations are possible, two of which are indicated by A and B. Even though the observed contact angle, θ, is quite different for these two configurations, the actual contact angle, θ_S, is the same.

The premise in the above analyses has been that Young's equation is obeyed. Recently, Young and Gauss's model has been challenged on the grounds that they assumed a constant value of the surface energy on each interface all the way to the contact line. However, it is known that the size of the region surrounding the interface (referred to as the *interfacial region*) that contributes to the surface energy extends many molecular diameters into the bulk, even when the mass-density changes almost discontinuously. If the thickness of the interfacial region is very small compared with any typical length scale, e.g. the radius of a drop or bubble, then it is reasonable to model the system with all of its "excess" energy concentrated on a surface having no thickness. However, in the case of a contact line, there exists a region within which the interfacial region associated with the three phase boundaries overlap (refer to Figure 4a). It is within this region about the contact line that the validity of modeling each interface with a constant surface energy and zero thickness has been questioned.

Lord Rayleigh (1890) was the first person to assess the effect of this region on the value of the contact angle. The molecular model that he used consists of a long-range[4] pairwise additive force-potential, ϕ, which is dependent only on the distance between molecules, and an "intrinsic pressure," P_i, to account for short-range repulsive forces of which he

[4] The term "long-range" refers to the fact that they affect material separated by distances over which continuum modeling makes sense; however, from a continuum point of view, these distances are very small.

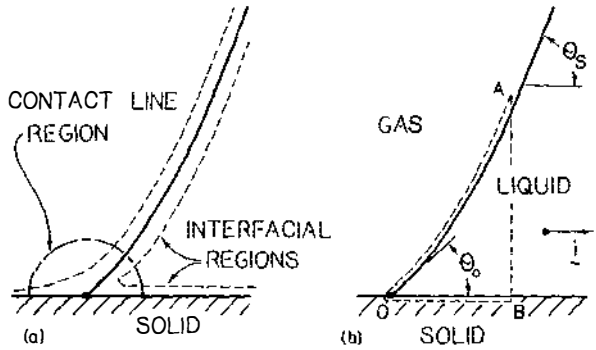

Figure 4 (*a*) The solid line represents the location of the abrupt change in mass-density in a system consisting of two immiscible fluids and a solid. The interfacial and contact line regions are enclosed within ---------, and ——— —, respectively. (*b*) The region enclosed by -------- denotes a fluid material body that extends outside of the contact line region at points *A* and *B*.

admitted little knowledge, and whose magnitude precisely balances the attractive forces in order to maintain the fluid at a constant mass-density. A balance of forces within the fluid yields:

$$0 = -\nabla P_i(\mathbf{r}) + \nabla \int_V \rho_F \rho \phi \left(|\mathbf{r} - \mathbf{r}'|\right) d\mathbf{r}',$$

where V denotes the volume of all the material that interacts with the fluid (when integrating over the solid $\rho = \rho_S$, and when integrating over the fluid $\rho = \rho_F$; however, within each phase the density, ρ, is constant), and $d\mathbf{r}'$ denotes a differential volume. The intrinsic pressure should not be confused with the hydrodynamic pressure appearing in the Navier-Stokes equation. Rayleigh calculated the surface tension from the rapid variation of P_i within the interfacial region.

The shape of the fluid-fluid interface was determined by balancing the forces acting on the material body enclosed within OAB (refer to Figure 4b). The points A and B were chosen sufficiently far from the contact line, O, so that they were well outside the contact-line region. The **i**-component of the force balance yields Equation (1); [refer to p. 405 of Rayleigh (1890)]. Thus, the fluid-fluid interface approaches a plane inclined at an angle θ_S to the horizontal, the same angle that appears in Young's equation, even though the interface may bend in the contact-line region and form a different angle, θ_0, with the solid surface.

Miller & Ruckenstein (1974), Jameson & del Cerro (1976), and del Cerro & Jameson (1976) examined the contact-line region from the same point of view as Rayleigh. However, they constrained the shape of the

interface between points O and A to be *planar*. Using different techniques and a specific potential:

$$\rho_F \rho \phi\left(|\mathbf{r}-\mathbf{r}'|\right) = \begin{cases} \dfrac{+\rho_F^2 \beta_{FF}}{|\mathbf{r}-\mathbf{r}'|^6} & \text{for } D < |\mathbf{r}-\mathbf{r}'|; \quad \mathbf{r}' \text{ is located in the fluid} \\ \dfrac{+\rho_F \rho_S \beta_{FS}}{|\mathbf{r}-\mathbf{r}'|^6} & \text{for } D < |\mathbf{r}-\mathbf{r}'|; \quad \mathbf{r}' \text{ is located in the solid} \\ 0 & \text{for } |\mathbf{r}-\mathbf{r}'| \leqq D \end{cases}$$

they derived an expression for the contact angle which is not Equation (1). This must be a consequence of requiring a planar fluid interface, since Rayleigh's derivation does not depend on the explicit form of $\phi(|\mathbf{r}-\mathbf{r}'|)$.

While Rayleigh's method of dealing with intermolecular forces is instructive, the statistical-mechanical treatment of liquids has advanced significantly in the last 30 years (Barker & Henderson 1976). One approach is to express the "hydrodynamic" stress tensor, $\mathbf{T}$, as the sum of a kinetic part and another part involving the intermolecular force potential that includes the long-range attractive as well as the short-range repulsive force (Irving & Kirkwood 1950). When summing these forces the short-range molecular structure of liquids is taken into account, i.e. within two to three molecular radii of any particular molecule the liquid has an ordered structure somewhat like a solid. Assuming no other force fields are present, static equilibrium requires a divergent-free stress tensor. The stress is sensitive to variations in the mass-density. Near phase boundaries such as the vapor-liquid interface, $\mathbf{T}$ becomes very anisotropic. It is this characteristic from which the surface tension is calculated (Kirkwood & Buff 1949).

Within this context, Berry (1974) has analyzed the shape of the fluid-vapor interface in the contact-line region. Numerous simplifying assumptions were made, some of which are known to give rise to a poor approximation of the stress field near vapor-liquid boundaries. It is interesting to note that in his final equations the stress tensor in the liquid near the solid is not anisotropic. In any case, Berry is able to show that there is only one interfacial shape with the property that it approaches a plane inclined to the horizontal away from the solid. The angle of inclination satisfies an equation that resembles Young's.

Saville (1977) has analyzed the problem numerically by simulating the dynamics of the molecules. Within a box, the trajectories of 400 to 1200 molecules were followed. A molecule in the box interacted with the entire wall according to a (9, 3) potential, and with another molecule

according to a Lennard-Jones (12, 6) potential. This technique enables one to "measure" numerically various equilibrium properties of the system that have not as yet been measured in the laboratory, e.g. σ_{LS} and σ_{GS}. Upon making independent evaluations of θ_S, σ_{LG}, σ_{LS}, and σ_{GS}, he concluded that Young's equation is not satisfied.

THE MOVING CONTACT LINE

Experimental Observations

Very little is known about the details by which one fluid displaces another at the moving contact line, either from a molecular or continuum point of view. Thus far, experimental investigations can be classified into two general categories: observations at various degrees of magnification of the shapes of menisci with the objective of measuring the dynamic behavior of the contact angle, and observations of the motion of dye marks and particles situated near the moving contact line with the aim of elucidating the displacement process from a continuum point of view. Though limited in scope, these experiments have revealed some interesting information.

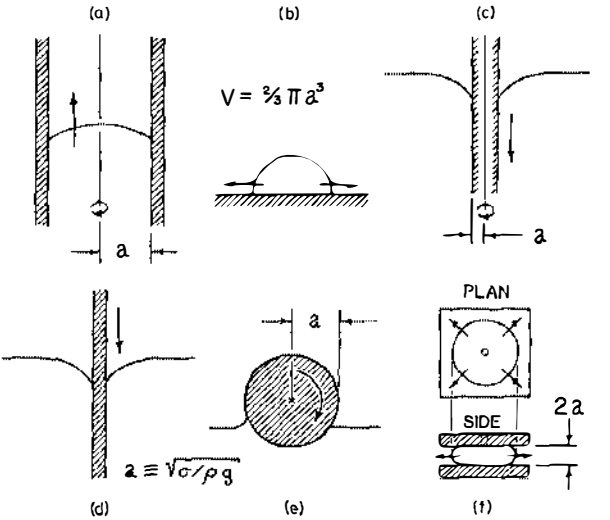

Figure 5 (*a*) The mutual displacement of two immiscible fluids through a capillary of radius *a*. (*b*) The spreading of a drop of liquid of volume *V* on a flat solid surface. (*c*) The submerging of a cylinder of radius *a* into a bath of liquid. (*d*) The submerging of a tape into a bath of liquid. (*e*) The rotation of a cylinder of radius *a* partially submerged into a bath of liquid. (*f*) The spreading of a liquid between two parallel plates in which the liquid is introduced through a hole in the center of the top plate.

MEASUREMENTS OF THE DYNAMIC CONTACT ANGLE If we recognize the fact that an analysis of any flow field in which the moving contact line plays an important role requires a boundary condition for the shape of the meniscus, it is not surprising to learn that the objectives of almost all experimenters in this field have been to determine the dynamic behavior of the contact angle. Although different geometries have been used, the dynamic contact angle is usually measured in the same way, by examining photographs of the menisci taken through a low-power microscope (at approximately 20 times magnification). The most well-known configurations are illustrated in Figure 5. The results of the various experiments, performed with different liquids and solids under various dynamic conditions, can be compared best when expressed in dimensionless form. The relevant dimensionless parameters are: the Reynolds number, $\mathrm{Re} \equiv Ua\rho/\mu$; the Bond number, $\mathrm{B} = \rho g a^2/\sigma$; the viscosity ratio, μ_1/μ_2; the capillary number, $\mathrm{Ca} \equiv U\mu/\sigma$; the Weber number, $\mathrm{We} \equiv \mathrm{Re} \cdot \mathrm{Ca}$; and the static contact angle, θ_S. Here, U is the speed of the contact line and a denotes the length-scale characteristic of each flow field (refer to Figure 5). The Bond number and the capillary number indicate the relative importance of gravity and viscosity as compared with surface tension in determining the shape of the meniscus.

A significant portion of the dynamic contact angle data has been obtained by observing flow through a circular capillary. For obvious reasons, treated and untreated glass has been the most popular solid, though some plastics have also been used. Almost all of these experiments have been performed under conditions of negligible Bond[5] and Reynolds numbers, and small capillary number. This gives rise to a meniscus shaped like a spherical cap with a radius whose size is determined by the dynamic conditions; the capillary number and the static contact angle are the only remaining parameters upon which it can depend. For a long time it was thought that the fluid-fluid interface is spherically shaped not only at its center, where it is observed, but also near its edge, i.e. near the moving contact line. Hence, the angle formed by the intersection of the spherical cap with the wall of the capillary has been interpreted as the actual dynamic contact angle. However, Hansen & Toong (1971) have pointed out that the viscous forces can play an important role in determining the shape of the meniscus in the immediate vicinity of the contact line, even at small values of the capillary number, e.g. $\sim 10^{-3}$. Consequently, the contact angle defined above, θ_M, is an

[5] The solution of the static shape of the meniscus given by Concus can be used to determine the maximum value of the Bond number below which gravitational effects are negligible.

apparent and not the actual contact angle, the latter being too difficult to measure. The angle θ_M can be readily be calculated from measurements of the distance between the plane containing the contact line and the apex of the meniscus, h, by the relationship:

$$\cos\theta_M \equiv [1+(h/a)^2]^{-1}\, 2h/a. \tag{2}$$

Hoffman (1975) has found an empirical correlation for the dependence of θ_M on Ca and θ_S (the static advancing contact angle), which fits remarkably well the behavior of numerous systems consisting of various oils displacing air through treated and untreated glass capillaries:

$$\theta_M = H\,(\mathrm{Ca}+H^{-1}(\theta_S)],$$

where H^{-1} is the inverse of H, i.e. $x \equiv H[H^{-1}(x)]$, and $H(0) = 0$ (refer to Figure 6). For example, if the static angle $\theta_S = 90°$, then the dynamic angle $\theta = 120°$ at Ca $\cong 5.4 \times 10^{-2}$. The main feature of this correlation is that θ_M is sensitive to the speed of the contact line, Ca, when θ_S is small, and loses its sensitivity as θ_S increases in value. While this correlation captures the general behavior of θ_M over its entire range, i.e. $0° < \theta_M < 180°$, the distance of some of the data points from the curve is too far to be attributed entirely to experimental error. That this correlation does not apply for all fluids is evidenced by the fact that it does not agree with the data of Blake & Haynes (1969).

Another system that has enjoyed some popularity consists of a small drop of liquid spreading on a flat horizontal solid surface (refer to Figure 5b). This configuration offers more flexibility than the capillary in that *any* solid material can be used; however, the fact that its flow field is unsteady is its most serious drawback. The conditions of the experiment

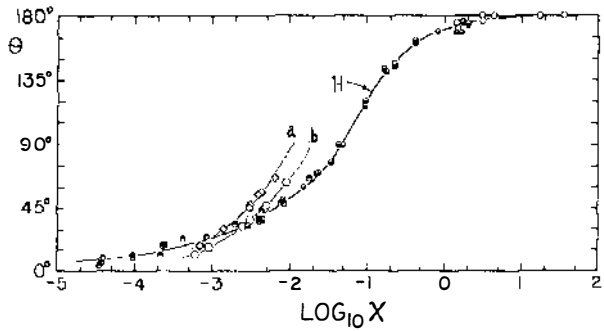

Figure 6 Hoffman's correlation is given by curve H, where $\chi \equiv \mathrm{Ca}+H^{-1}(\theta_S)$. The spreading of two drops, identical in every way except for their volume, have been measured by Schonhorn, Frisch & Kwei. The curves a and b refer to drops having volumes of 0.0058 and 0.021 cm^3, respectively, where $\chi \equiv$ Ca.

and the types of observations are very similar to that of the capillary. Only drops of sufficiently small volume, V, are used so that both gravity and inertia are negligible, and the capillary number is small. Under these conditions the drop appears to be shaped like a spherical cap whose radius is a function of time. The apparent contact angle, θ_{APP}, can be calculated upon measuring the instantaneous radius, r, of the circular area where the drop wets the solid, along with either the volume of the drop, or the instantaneous height of the apex of the drop above the surface of the solid, h, by either of two formulae:

$$\frac{r^3}{V} = \frac{3}{\pi} \frac{(1+\cos\theta_{APP})\sin\theta_{APP}}{(1-\cos\theta_{APP})(2+\cos\theta_{APP})},$$

or,

$$\frac{h}{r} = \frac{1-\cos\theta_{APP}}{\sin\theta_{APP}}.$$

Unfortunately, probably due to the fact that the flow field is unsteady, there has been a general lack of understanding as to the type of data that characterize the spreading properties of the materials, i.e. data, though measured in one geometry, which can be used to characterize the spreading of the same liquid in any geometry. As a consequence, it is common to find an incomplete reporting of experimental results. For example, one might find the time dependence of θ_{APP} presented without any specification of the volume of the drop, or the dependence of θ_{APP} on the time rate of change in the size of the wetted area of the drop on the solid without the explicit variation of the size of the wetted area with time. Not only do these not represent properties of only the materials of the system, they are insufficient for calculating the dependence of θ_{APP} on the speed of the contact line. The confusion in the interpretation of results that exists when using this particular geometric configuration can be illustrated by the very interesting work of Schonhorn, Frisch & Kwei (1966) and Kwei, Schonhorn & Frisch (1968). Upon observing the spreading of a combination of two liquids on three different solids at various temperatures, they found that all of their data of r/a (or $\cos\theta_{APP}/\cos\theta_S$) as a function of the dimensionless time, $t\sigma/L_W\mu$, could be represented by a single curve. The adjustable parameter L_W, which has dimensions of length, they found to be constant for a specific liquid-solid combination, i.e. it is independent of both the temperature of the system and the volume of the drop. Consequently, they have proposed that their empirically determined relationship of $\cos\theta_{APP}/\cos\theta_S$ versus $t\sigma/L_W\mu$ is a characteristic of only the material of the system. In fact, there

are papers in the literature that use this relationship as a boundary condition for the spreading of the same liquids in different geometric configurations. However, if the experimental data are recast in the form of $\cos \theta_{APP}$ versus Ca, then one finds that they contain a dependence on the volume of the drop (refer to Figure 6) and hence cannot be considered independent of the geometric configuration from which they were measured.

The configuration illustrated in Figure 5c, consisting of a circular cylinder entering a large bath of liquid, differs from the previous two cases in many ways. To begin with, even when the Bond number is small, gravity cannot be neglected since it is entirely responsible for the horizontal planar shape of the liquid-air interface away from the moving cylinder. Experiments [Inverarity (1969) and Schwartz & Tejada (1972) being the most notable] have been performed on a variety of solids using numerous liquids with the parameters varying over a wide range of values: $0 \lesssim B \lesssim 1$; $10^{-5} \lesssim Ca \lesssim 10^{+2}$; $10^{-4} \lesssim Re \lesssim 10^{+3}$. Unlike the capillary and spreading drop, the interface does not closely resemble a static configuration; hence, the only way of obtaining the dynamic contact angle is by drawing a line tangent to the meniscus at the contact line on an enlarged photograph and measuring the angle that it forms with the solid. It is not uncommon to find within one set of data of dynamic contact angle versus Ca that the Reynolds number varies from a small to large value as Ca increases in magnitude. This implies that the flow field below the deformed portion of the meniscus, usually within a distance of approximately $5\sqrt{\sigma/\rho g}$ from the moving contact line, is dominated by viscous forces when Ca is small, and inertia when Ca is large. Inverarity is able to describe all of his data obtained with organic liquids with one "master curve" (the data scatters to within $\pm 6°$ of the curve, while he claims $\pm 2°$ reproducibility); this curve has the same general behavior as Hoffman's correlation. However, he finds that water, a polar liquid, exhibits anomalous behavior; its contact angle approaches a limit (its value depends on the solid material) of less than 180° as Ca increases in magnitude. Schwartz & Tejada (1972) obtain curves of the dynamic contact angle versus Ca which have a discontinuity in their slopes for some organic fluids. This usually occurs at Re between 5 and 20. While all of the investigators tend to attribute their unusual observations to a change in the mechanism of spreading at the moving contact line, it is not at all obvious that their origins are not hydrodynamical.

The primary objective of examining a tape entering a bath of liquid (refer to Figure 5d) has been to determine the conditions of incipient air entrainment. Burley & Kennedy (1976a,b), using liquids with various viscosities and different types of plastic tapes, have determined an

empirical formula for the speed of the contact line at which this occurs. Entrainment was characterized by a dynamic contact angle at 180°. For each liquid this was achieved at a particular contact-line speed independent of the type of tape used. Although Reynolds numbers greater than one were typical throughout their investigation, the dependence of the dynamic contact angle on Ca followed the same general trends of Inverarity's master curve and Hoffman's correlation. Interestingly, they found that fluids with viscosities greater than 4.5 poise always began entraining air at a contact-line speed of 9.5 cm sec^{-1}. The less viscous fluids began entraining air at Ca within the interval $[0.21, 0.83]$, and this always occurred when the contact line reached a depth of 0.4 cm below the undisturbed level of the liquid surface.

One of the earliest experimental studies of the dynamic contact angle was performed by Ablett (1923) using a horizontal rotating waxed cylinder of about three inches in diameter partially submerged in tap water (refer to Figure 5e). His procedures consisted of rotating the cylinder at a given constant frequency and then filling the surrounding tank with water to the precise level that rendered the meniscus on one side of the cylinder uniformly horizontal all the way up to the contact line. The dynamic contact angle was assumed to be the angle formed between the horizontal and the tangent to the cylinder at the contact line and was calculated from the measured value of the height of the water-air interface relative to the lowest submerged portion of the cylinder. He found that the advancing (receding) dynamic contact angle increased (decreased) in size until the contact line reached a speed of 0.04 cm sec^{-1} [corresponding to $Ca \approx 6 \times 10^{-6}$ and $Re = (\sigma/\rho g)^{1/2} \times U\rho/\mu \approx 1$] and the contact angle achieved a value of 113° (96°), and did not vary any more as the speed of the contact line was increased ten fold.

Elliott & Riddiford (1967) have introduced a novel geometry (refer to Figure 5f) which consists of pumping a liquid through a hole in the center of one of two parallel plates separated by a distance of 0.15 cm. As the liquid flows radially away from the hole it displaces a second immiscible fluid. The volumetric flow rate varies in a predetermined way so that the speed of the meniscus remains constant. The Reynolds number based on the separation of the plates was less than 0.25 and the capillary number varied within the interval $[10^{-7}, 10^{-5}]$. They have examined advancing and receding contact lines of water displacing oil and water displacing air saturated with its own vapor on siliconed glass and polyethylene surfaces. Water advancing on siliconed glass was the only material system that exhibited a limiting angle less than 180° (115° at $Ca \simeq 10^{-6}$). They found it difficult to perform experiments by withdrawing the liquid due to the erratic and unsteady motion of the

receding contact line. While Elliott & Riddiford attributed this to non-uniform molecular behavior, Wilson (1975), who has performed a linear hydrodynamic stability analysis, has presented convincing evidence that at least part of the difficulties arise from an instability in the flow field.

OTHER OBSERVATIONS As early as 1919, Hardy demonstrated that drops of certain liquids when placed on a solid, even though they undergo no visible change in shape, emit a very thin invisible film along the surface of the solid. He was able to detect its presence by measuring a significant change in the value of the static friction of the surface. Drops of acetic acid on glass (it is important that the air is dry) were found to emit a film, while drops of castor oil and paraffin did not. The terms *primary* and *secondary* were coined to distinguish the invisible film from the rest of the drop. Stating that he was unable to conceive of a mechanism by which the liquid at the leading edge of the primary film could move forward along the immobile solid, Hardy proposed that the initial wetting of the solid, i.e. the motion of the leading edge of the primary film, occurs by a process involving a continual condensation of vapor.

Equipped with an ellipsometer and an interferometer, Bascom, Cottington & Singleterry (1964) investigated the characteristics of the primary and secondary films from a more quantitative point of view. They examined the behavior of various nonpolar liquids on clean, smooth metal surfaces in the presence of both saturated and unsaturated air. Three methods proved to be successful for detecting the presence and the size of the primary film: noting the form of condensation patterns of humid air blown onto the solid, observing the anomalous behavior of a small drop of a different liquid placed on the film, and measuring the thickness of the film with the ellipsometer. They were able to come to the following conclusion: For all the liquids they studied (all were chosen because they exhibit a zero contact angle from macroscopic observations), a *primary* film was always present, i.e. making the air saturated or unsaturated with vapor, roughening the surface, and ultra purifying the liquids did not eliminate the primary film, although it did affect the speed at which it spread over the solid. Squalane on stainless steel exhibited a primary film with a thickness of approximately 20 Å and a leading edge that moved at speeds ranging from 0.03 to 1.0 μm sec^{-1}. However, whether or not the *secondary* film would spread over primary film was greatly influenced by the above-mentioned factors. They found that the most important factor responsible for the spreading of the secondary film was the presence of a gradient in surface tension induced by a variation in concentration of very slight amounts of

volatile trace contaminants. It is interesting to note that for liquids with a high molecular weight, which always contain a distribution of molecular sizes, the molecules with slightly lower than average molecular weight play the same role as trace impurities. And finally, by finding only a few angstroms of material adsorbed onto a metal surface that was placed parallel to a squalane-air interface separated by a distance of 0.08 cm for a period of 72 hours, they concluded that the leading edge of the primary film advances by the migration of liquid along the solid, and not, as suggested by Hardy, by an evaporation-condensation scheme through the air. They refer to this transport at the leading edge of the primary film as *surface diffusion*; nothing specific, other than the above, is presented to justify the use of this terminology.

One of the most exciting tools to emerge in recent years for examining the shape of the meniscus close to the contact line under dynamic as well as static conditions has been the scanning electron microscope. Even though its degree of resolution is about the same as a good light microscope (approximately 0.5 μm), an enhanced picture is obtained as a consequence of its very large depth of field. Oliver & Mason (1977), from examinations of drops of polymers and oils on surfaces of various textures, have observed large variations in the value of the contact angle along the contact line, which then blended into a smooth meniscus at short distances. For example, on a surface made of close-packed latex spheres, the apparent contact angle, i.e. that measured under low magnification, was 20°, while the contact angle as seen with the scanning electron microscope appears to closely approximate 0° at a number of places.

Flow visualization, one of the oldest experimental techniques, has also been used to study the displacement process. Although a number of people have referred to liquid spreading over the surfaces of solids as *sliding*, those who have used small particles and dye marks to visualize the flow have referred to it as *rolling*. Yarnold (1938) described a glob of mercury moving down a gently sloping plane as rolling, based upon his observations that dust particles on the air-mercury interface traveled forward more quickly than the fluid in the interior. Schwartz, Rader & Huey (1964), by placing a dye mark at one end of the index of liquid in a capillary, observed that the liquid rolled away from the wall at the rear and towards the wall at the front. That at least one of the two adjacent displacing fluids undergoes a rolling-type motion was documented by Dussan V. & Davis (1974) by photographing the motion of dye marks in systems consisting of various combinations of immiscible fluids; these included liquid-air systems with both advancing and receding contact

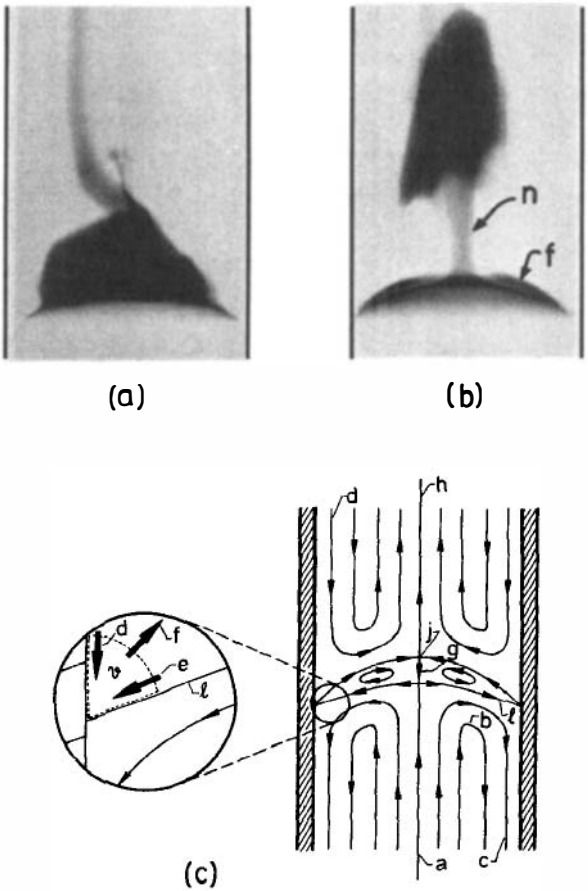

Figure 7 Glycerine, the lower fluid, is displacing oil through a Plexiglas tube. Viewed from a frame of reference at rest with respect to the glycerine-oil interface, *l*, the walls appear to be moving with a constant downward velocity. For this system it is the glycerine that undergoes the rolling motion. Glycerine flows upward at the center, *a*, radially outward near the glycerine-oil interface, *b*, and downward close to the wall, *c*. The oil is the fluid with the more complex motion. Focusing attention on the motion of the oil near the contact line we see that oil must be dragged into *V* at *d* and *e* due to the motion of the wall and the glycerine, respectively. Conservation of mass requires an outward flow at *f*. The motion of the oil far above the glycerine-oil interface is similar to that of the glycerine. Oil is dragged downward near the walls, *d*, and upward at the center, *h*. As a consequence of the axial symmetry, there is a bolus of oil "captured" within *f* and *l* near the glycerine-oil interface. This creates a stagnation-point flow within the oil at *j*, and a downward flow at *g*. The motion of the oil is visualized by injecting oil containing a black dye near the glycerine-oil interface (*a*). Note that the glycerine-oil interface billows into the oil. After a while, (*b*), dye outlines the bolus. The necking of the dye at *n* is evidence of the stagnation point within the oil (Dussan V. 1977).

lines and liquid-liquid systems. In addition, they found that the fluid adjacent to the one that rolls exhibits a more complex flow pattern. Immiscible fluid displacement through a capillary is illustrated in Figure 7.

Analysis and Modeling

One of the more conceptually difficult aspects associated with one viscous fluid displacing another, whether it be a liquid or a gas, over a solid surface, is envisioning from a continuum point of view the mechanism by which this occurs. For a long time it was thought that if the fluids obeyed the no-slip boundary condition at the surface of the solid then a nonequilibrium condition originating at the contact line could not cause the contact line to move. This feeling was further reinforced by the fact that analyses of flow fields containing moving contact lines predicted the presence of an infinite force. Two separate concepts are involved: Is it kinematically possible for two fluids not to slip on the solid surface in a flow field containing a moving contact line? Why do the analyses contain an infinite force and what must be done to remove it? Whereas a fairly complete answer already exists to the first question, it does not to the second, in part because of a lack of knowledge of the physical process by which the contact line moves. However, analyses over the past eight years have indicated a procedure by which a well-posed boundary-value problem may be formulated from a fluid mechanical point of view for which this specific knowledge does not seem to be necessary.

KINEMATICS: COMPATIBILITY BETWEEN SPREADING AND NO-SLIP That the no-slip boundary condition and a moving contact line are compatible from a kinematic point of view has been demonstrated by Dussan V. & Davis (1974). The key, they found, lay in the realization that the terms *no-slip* and *adherence* are not equivalent (refer to Figure 8). The rolling motion of one of the fluids near the contact line created by a nonequilibrium value of the contact angle is somewhat analogous to a ball rolling down an inclined plane: both can move even though the no-slip boundary condition is satisfied at the surface of the solid. Whether or not this type of motion actually occurs can only be determined from studying its dynamics.

The flow field illustrated in Figure 8 has an unusual characteristic, as indicated by Dussan V. (1976a) in her detailed examination of the kinematic boundary condition. It shows that surfaces bounding fluid bodies need not always consist of the same material points. In this particular example, the surfaces *DOB* and *COB* bound the entire body of fluid, and one of the two fluids above the solid, respectively; however, neither is a material surface. One of her main conclusions is that: if the

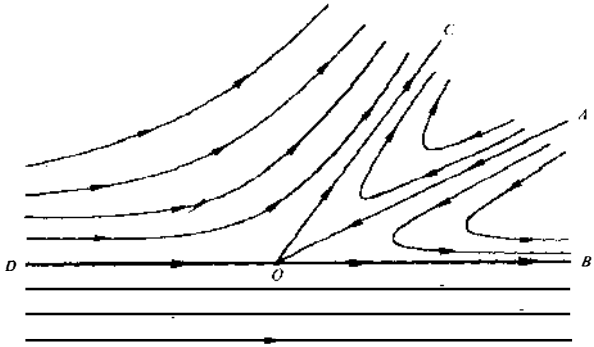

Figure 8 The solid is located below *DOB* and the fluids, above. Surface *DOC* bounds the fluid which is rolling off the solid and surface *COB* bounds the other fluid. The fluid point at *D* moves to *O* in a finite interval of time without slipping, whereupon it leaves the surface and arrives at *C* at some later time. The no-slip boundary condition is obeyed; however, the fluid does not adhere to the surface of the solid (Dussan V. 1976a).

fluid velocity, $\mathbf{u}(\mathbf{x}, t)$, is smooth enough to guarantee a unique solution to the associated initial-value problem, $d\mathbf{x}/dt = \mathbf{u}(\mathbf{x}, t)$ with $\mathbf{x} = \mathbf{x}_0$ at $t = 0$, then surfaces bounding material bodies are material surfaces.

DYNAMICS Flow fields containing moving contact lines also contain free surfaces. Since their location is not known a priori, they introduce additional difficulties into the associated boundary-value problem. Over the years various techniques have been developed for dealing with this situation. The methods that have most frequently been used for analyzing flow fields with moving contact lines consist of either performing a domain perturbation, or making the lubrication approximation. Those analyses that have modeled the fluids as Newtonian and incompressible, and have used the no-slip boundary condition at the solid surface, *all* have singularities at the contact line, i.e. the approximate solutions are not uniformly valid there.

When making the lubrication approximation, the singularity shows up in the solution for the shape of the meniscus by always forming a 90° contact angle at the solid (Buckmaster 1977). Since the lubrication approximation is used primarily for the spreading of thin layers of liquid within which the velocity vector lies almost parallel to the local tangent to the solid surface, obtaining a 90° contact angle implies that the approximate solution is invalid close to the contact line. Only when the value of the dynamic contact angle has little affect on the overall shape of the meniscus can this singularity be ignored, e.g. the spreading of a relatively large drop (Lopez, Miller & Ruchenstein 1976, Smith 1969).

When the meniscus lies close to a coordinate surface, domain perturbation has been a convenient technique. Huh & Scriven (1971) have examined the mutual displacement of two viscous fluids along a flat solid surface in which the fluid-fluid interface was assumed to be a plane. It is not clear whether they intended this to represent a plate entering a bath of liquid at the specific angle that makes the fluid-fluid interface appear flat all the way up to the contact line (as in Ablett's experiment, except he used a circular cylinder), or to describe the local motion of the fluids close to any moving contact line. The reason for this is that they never present any criteria for determining the angle that the fluid-fluid interface makes with the solid surface. It cannot be the actual contact angle because the solution for the first-order correction of the shape of the interface is singular at the contact line. On the other hand, it does not represent the angle that the interface far from the solid makes with the wall because the solution for the interface shape (their Equation 30) does not asymptotically approach a plane far away from the contact line. Their solution also contains the unrealistic characteristic that the fluids exert an infinite force on the solid. However, close to the contact line, their streamlines look very much like those given in Figures 7 and 8. They attributed the deficiencies in their solution to the kinematic incompatibility between the no-slip boundary condition and the moving contact line; we have already seen that this is not the cause.

The principal drawback with any velocity field having the general characteristics shown in Figure 8 is that it must be multi-valued at the contact line, i.e. the value of the velocity vector at any point on the contact line depends upon the direction from which it is approached. It is this characteristic along with the assumptions that the fluids are Newtonian and incompressible that gives rise to the infinite-force singularity at the moving contact line (Dussan V. & Davis 1974). This is a *dynamic*, as opposed to kinematic, *incompatibility* among the modeling assumptions. The singularities in the above-mentioned analyses are *not* a consequence of the approximation techniques but are inherent in the original boundary-value problem. In order to transform this into a well-posed physical, as well as mathematical, problem the model of the fluids must be altered in such a way that the singularity is removed.

It is difficult to model a phenomenon for which there has been very little direct experimental measurement. It also seems naive to expect one model to cover all situations. For example, with slowly spreading liquids it remains unclear whether the contact line should be identified with the leading edge of the primary or secondary film. To choose the former implies a willingness to perform a detailed analysis of a fluid whose stress tensor is unknown, not to mention anisotropic, due to the

proximity of any point within the fluid to both the fluid-fluid and fluid-solid interfaces. A more realistic approach would seem to favor incorporating the primary film into the model of the surface of the solid and locating the contact line at the leading edge of the secondary film. Modeling very thin layers of material as a surface phase or as part of the surface of the solid is not not a novel idea. For years it has been known that the attractive force of a solid can cause molecules to adsorb onto the surface. Molecules adsorbed from the vapor phase onto a surface in amounts of less than one molecular layer have been successfully modeled as a two-dimensional fluid (Glandt, Myers & Fitts 1978). An adsorbed layer was always present on the interface of the *vapor-solid* boundary in Saville's (1977) molecular dynamics calculations for determining the static contact angle. In addition, Zisman (1964) regarded the surface of a solid retracting from a bath of "autophobic" liquids as *dry*, even though the surface retained an adsorbed layer of molecules. Hence, it does not seem unreasonable to model the primary film, or the molecules of the displaced fluid that might have remained at the solid-displacing fluid interface as surface phases. In other words, eliminating the singularity at the contact line by not permitting it to exist in the boundary-value problem because the displacement process is being treated as a coating flow does not necessarily make it more tractable, nor is it encouraged by models already used by chemical physicists.

There are many ways of altering the model of the fluid near the contact line with the aim of removing the singularity; however, relieving the no-slip boundary condition has been the only one pursued thus far. Various models have been proposed. Hocking (1976) has presented a local continuum model of the displacement process and has derived expressions for the slip coefficient, β, which appears in the often-suggested boundary condition: $\mathbf{t}(\mathbf{t}\cdot\mathbf{Tn}) = \beta \boldsymbol{u}\mathbf{t}$; where $\mathbf{t}(\mathbf{t}\cdot\mathbf{Tn})$ is the tangential component of the surface-traction vector (equal to $\mu\partial u/\partial Y$, where Y denotes the direction perpendicular to the surface), and $\boldsymbol{u}\mathbf{t}$ is the velocity of fluid at the wall ($Y = 0$). The surface of the solid, although modeled as a plane, was assumed to be scratched with periodic straight grooves shaped like a sine wave. The only case investigated consisted of fluids moving in a direction perpendicular to the generators of the surface. The contact line, he conceived, moves discontinuously as a consequence of the fluid-fluid interface making contact with the solid only at the crest of the grooves, even though from a macroscopic point of view its motion may appear to be smooth. The expression for β to be used at the solid-displaced fluid interface was determined by requiring the velocity fields of the following two boundary-value problems to approach the same form above the surface: (*a*) the displaced fluid is semi-infinite in extent, the

surface of the solid is planar, the fluid obeys the above-mentioned slip boundary condition at the surface ($Y = 0$), and the fluid flows parallel to the wall with a constant gradient ($\partial u/\partial Y =$ constant independent of X as $Y \to \infty$); (*b*) the same as above except that the fluid obeys the no-slip boundary condition on the grooved surface. The only differences in procedure for determining β at the solid-displacing fluid surface was to substitute "displacing" for "displaced," and to replace the fluid below the height of the crest of the grooves in (*b*) by the displaced fluid which was entrapped as the contact line moved by. It is understandable why Hocking has restricted his analysis to such an idealized situation; however, the appropriateness of the assumption that $\partial u/\partial Y \to$ constant independent of X as $Y \to \infty$ in the derivation of β is not obvious.[6] Hocking also uses this slip boundary condition to analyze the mutual displacement of two immiscible viscous fluids through a capillary and between two parallel plates in which the fluid-fluid interface is flat and forms a 90° contact angle to first approximation (Hocking 1977). His analysis, as with all of the others to be discussed, represents the leading term of a domain perturbation and is restricted to small Reynolds, capillary, and Bond numbers. One of his most important contributions is to demonstrate that flow fields containing contact lines can be analyzed by the method of matched asymptotic expansions, the small parameter being the ratio between the length scales characterizing the slip boundary conditions μ/β, and the overall geometry, a. The limit as this ratio approaches zero is singular since it represents the original problem, i.e. this gives the no-slip boundary condition over the entire wall. The domain of the fluid separates into two parts: the *inner region*, located in the immediate vicinity of the contact line, within which the dynamics of the fluids is sensitive to the slip boundary condition; the *outer region*, the remaining fluid, where the geometry plays an important role but fluid does not slip along the wall. The flow field presented by Huh & Scriven (1971) turns out to represent the motion of the fluids in the overlapping region, i.e. the region where both the inner and the outer expansions are valid. From a physical point of view, Hocking was primarily concerned with determining the force exerted by the fluid on the surface of the solid. He found that not only was this slip boundary condition sufficient to remove the infinite-force singularity, but, for a reasonable range of slip coefficients, the pressure drop needed to cause two immiscible viscous fluids to flow through a capillary of length

[6] Upon examining the solution of the flow field near the contact line in which the boundary condition $\mathbf{t}(\mathbf{t}\cdot\mathbf{Tn}) = \beta u\mathbf{t}$ has been used, it is found that the tangential component of the surface-traction vector changes rapidly, dropping to about 1/4 the value it has at the contact line at a distance equivalent to only two grooves away.

greater than $100a$ can be approximated fairly well by Poiseuille flow. In other words, besides removing the singularity, the slip boundary condition plays a secondary role in determining the dynamics of the fluids.

In a sense, this last conclusion is not surprising when viewed in terms of West's formulation (refer to the Introduction) for calculating the pressure drop down the capillary. The value of the apparent contact angle, the angle in West's equation, is controlled by the dynamics of the fluid near the contact line. Even though the actual contact angle may be exactly 90°, as Hocking assumes, the apparent contact angle can take on any value between 0° and 180°. Its value depends on the choice of slip length. Hence, the maximum affect that the flow near the contact line can have on the pressure drop is $2\sigma/a$.

Huh & Mason (1977) propose a slip boundary condition based on a physical model of the motion of the molecules at the gas-liquid interface. As the molecules of the liquid come into contact with the solid at the moving contact line (the liquid is assumed to roll onto the solid), they are not oriented and require a finite interval of time, τ, before attaching themselves to the surface. During τ they experience no drag force by the solid; however, after τ, they do not slip along the surface. Viewing the molecules from a frame of reference at rest with respect to the contact line, Huh & Mason postulate a slip boundary condition of the form:

$$\begin{aligned} &\mathbf{t}\cdot(\mathbf{Tn}) = 0 \quad \text{for} \quad 0 < Z < l, \\ &\mathbf{u} = U\mathbf{t} \qquad \text{for} \quad l < Z, \end{aligned} \tag{3}$$

where $U\mathbf{t}$ is the velocity of the wall, Z is the distance from the contact line along the wall, and $l = U\tau$. They perform two analyses of the displacement of a gas by a liquid through a capillary within which the meniscus is assumed almost flat; first with the above boundary condition, and then with the one used by Hocking. As with Hocking, they use the method of matched asymptotic expansions; however, in addition to calculating the force exerted by the fluid on the solid, they determine the first-order correction to the shape of the interface. Both slip boundary conditions give rise to a bounded force, and a nonsingular equation for the shape of the meniscus. Unfortunately, the solution to the latter introduces a parameter whose value is not known: the dynamic contact angle. Huh & Mason's solution supports the findings of Hansen & Toong (1971), that almost the entire meniscus is shaped like a spherical cap, deviating significantly from that shape only near the contact line where the viscous forces are important. Huh & Mason also determined the dependence of the experimentally measurable apparent contact angle—the angle the

interface would make with the wall if it were shaped like a spherical cap all the way to the contact line [refer to Equation (2)]—on the capillary number, the actual dynamic contact angle, and the slip length, but they have difficulty comparing it with experimental data because of the fact that the values of the last two parameters are unknown. It is interesting to note that the flow field obtained with the slip boundary condition expressed in Equation (3) *does not* have the characteristics of the physical model that motivated its formulation. Material points located on the gas-liquid interface *never* arrive at the moving contact line, and the contact line always consists of the same material points, i.e. the liquid doesn't undergo a rolling motion at the moving contact line.

It is evident that the selection of slip boundary conditions is endless. In an attempt to assess the affect different models have on the overall dynamics of the fluid, Dussan V. (1976b) has investigated the flow field produced by a plate entering a large bath of liquid using three specific models, all of which were chosen entirely from mathematical and kinematical considerations. All the models were required to have two characteristics. In order to remove the singularity, it was necessary to assume that the velocity of the fluid instantaneously at the contact line and the velocity of the contact line were the same (Dussan V. & Davis 1974). Far away from the contact line, the velocity of the fluid at the wall approached the velocity of the wall, i.e. the fluid approached the no-slip boundary condition. In the region over which the transition in behavior took place, the size of which was defined to be the slip length, each model was different. Since the dynamics of the fluid is most sensitive to conditions at the contact line, the criterion for choosing the models was based upon the value of du/dZ evaluated at the contact line, and each model assumed one of the following values: 0, 1, ∞ [the velocity $u(0)$, having already been specified]. Explicit solutions were obtained. As might have been anticipated, the flow field very close to the contact line was different for all three cases; however, they were identical when examined on a length scale that characterized the overall geometry of the fluids, in this case, $(\sigma/\rho g)^{1/2}$. That is to say, the value of the slip length and the dynamic behavior of the contact angle were the only characteristics of the slip models that affected the shape of the meniscus and the force exerted by the fluid on the plate. The details of $u(Z)$ within the transition region were not important. The diversity represented by these three models can be appreciated by examining the slip coefficient, $\beta(Z)$, which would have to be used if the boundary condition were instead expressed in the form $\mathbf{t}(\mathbf{t}\cdot\mathbf{T}\mathbf{n}) = \beta(Z)u\mathbf{t}$ (refer to Figure 9). Note that the behavior of β is vastly different among the three models both near and far away from the contact line.

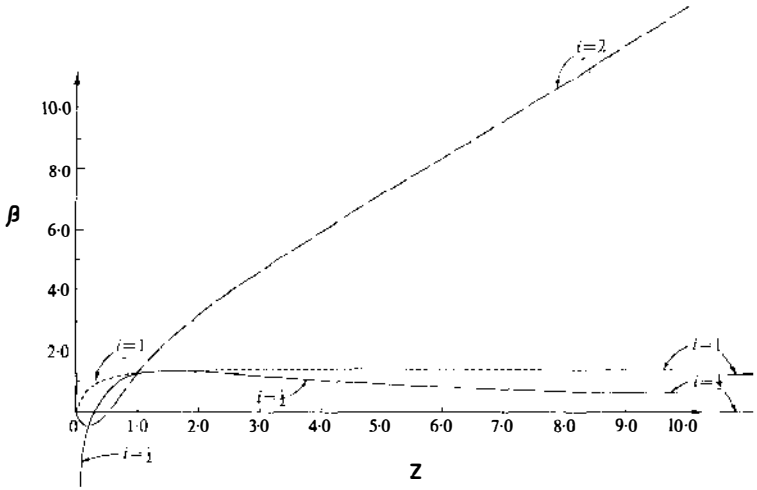

Figure 9 The slip coefficient corresponding to the models in which du/dZ, at $Z = 0$, equals 0, 1, and ∞ are given by $i = 2$, $i = 1$, and $i = 1/2$, respectively. The contact line is located at $Z = 0$ (Dussan V. 1976b).

An unfortunate conclusion to the above analyses is that the physical mechanism by which the contact line moves along a solid surface cannot be inferred by measuring such quantities as the shape of the meniscus or the force necessary to cause the fluids to move, since totally different slip models give rise to the same overall flow field. It would be informative if an approximate value of the slip length could be deduced: 10 Å would indicate the importance of long-range molecular forces, while 1000 Å might suggest a mechanism similar to Hocking's. But this is not possible because two unknown parameters, the slip length and the dynamic contact angle, appear in the results. On the other hand, if the primary interest is in the overall flow field, i.e. the flow in the outer region, then a detailed knowledge of the displacement process is probably not necessary. A close examination of the analyses of Hocking, Huh & Mason, and Dussan V. reveals that all the reported experimentally measurable quantities depend only on *one* parameter: $-4\pi^{-1}\,\mathrm{Ca}\ln L_S + \theta$.[7] Another feature is that they have the same velocity field in the intermediate region, i.e. no known constants are determined by matching the inner and the outer velocity fields. The shape of the meniscus is the only quantity in the outer region that is affected by the dynamics of the fluid

[7] This is based on analyses which assume that the capillary number is small, the contact angle, $\theta(U)$, is close to 90°, and only one viscous fluid is present. Hocking does not have the unknown $\theta(U)$ in his results because he assumes it is exactly 90°. In Hocking, and Huh & Mason, L_S is either $2\mu/\beta$ or l.

in the inner region. Hence, it is through the shape of the meniscus that the dynamics of the fluid in the inner region affects the overall flow field.

Kafka & Dussan V. (1978) have taken advantage of the above observations and have shown that the flow field can be formally separated into two parts. This is accomplished by introducing into the analysis θ_I (referred to as the intermediate angle), the angle formed between the vector tangent to the meniscus at a distance r_I from the contact line and the vector tangent to the wall. The distance r_I is specifically chosen so that it is imbedded well within the intermediate region.[8] Since the only link between the inner and outer regions is the shape of the meniscus, by knowing the dynamic behavior of θ_I, the flow field in the outer region can be calculated. This approach was originally suggested by Hansen & Toong (1971) although their justifications were different. For the case of two immiscible viscous fluids moving through a capillary with an almost flat fluid-fluid interface, Kafka & Dussan V. find

$$\theta_M = \theta_I - \frac{U}{\sigma}\left\{(\mu_1+\mu_2)\left[1.273 \ln\left(\frac{r_I}{a}\right) + 2.10\right] + \right.$$
$$\left. + \frac{\mu_1\mu_2}{\mu_1+\mu_2}\left[3.471 \ln\left(\frac{r_I}{a}\right) + 8.87\right]\right\},$$

where θ_M is the experimentally measurable apparent contact angle defined by Equation (2). The angle θ_I can be calculated from the above equation along with experimental data on the dynamic behavior of θ_M. The advantage of knowing the dynamic behavior of θ_I, compared to θ_M, is that it is only a property of the materials of the system and can be used as a boundary condition in any spreading problem, while θ_M depends on the geometry of the system in which it is measured. On the other hand, it is of scientific interest to determine whether or not a specific model of the displacement process at the moving contact line is appropriate for a specific material system. To do this, the motion of the fluid in the inner region—free from complicated geometry effects—need only be analyzed, and the behavior of θ_I determined. For example, assuming a specific slip model, they derive

$$\theta_I = \theta + \frac{U}{\sigma}\left\{(\mu_1+\mu_2)\frac{4}{\pi}\left[1 - \frac{\mu_2}{\mu_1+\mu_2}\ln\frac{L_{s_1}}{L_{s_2}} + \right.\right.$$
$$\left.\left. + \ln\frac{r_I}{L_{s_1}}\right] + \frac{\mu_1\mu_2}{\mu_1+\mu_2}\frac{64}{\pi(\pi^2-4)}\left[1 + \ln\frac{r_I}{(L_{s_1}L_{s_2})^{1/2}}\right]\right\},$$

[8] Strictly speaking, the intermediate region is not located at a fixed position in space, but rather has meaning only in an asymptotic sense when matching takes place.

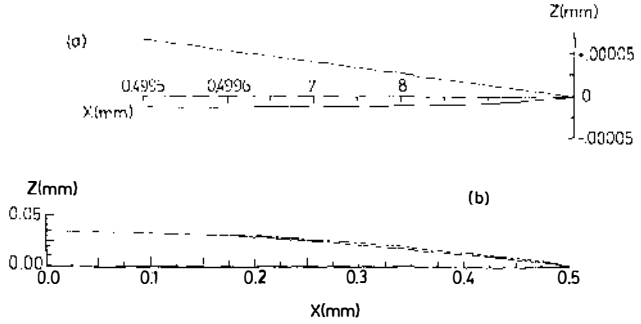

Figure 10 The shape of the meniscus for the case of $\mu_2 \ll \mu_1$ and Ca = 0.002, as observed from a macroscopic point of view, is given in (b). The position $X = 0$ corresponds to the center of the capillary and its inside surface is located at $X = 0.5$ mm. The curve ——— – ———, represents a spherical cap, and it is evident that the solution ———, although different, closely approximates it. The angle that the curve ——— – ——— makes with the wall is θ_M, and for this example $\theta_M = 98°$. On close examination of the contact line region (a), we find that the shape of the meniscus ——— differs from the spherical cap ——— – ———. The actual contact angle, θ, is 82°. It has been assumed that $\theta_I = 90°$ at $r_I = 5 \times 10^{-4}$ mm (Kafka & Dussan V. 1978).

where L_{S_1} and L_{S_2} are the slip lengths associated with the two fluids. It is necessary but not sufficient for the derived expression of θ_I to agree with the one obtained from experimental measurements of θ_M in order for the model to be valid. Note that when only one viscous fluid is present, θ_I depends directly on the term $-4\pi^{-1}$ Ca ln $L_S + \theta$. The parameter θ_I can always be eliminated by combining the above two equations; the resulting expression is the same as that obtained from a properly matched-asymptotic solution. The role of the three angles—θ, θ_I, and θ_M—is illustrated in Figure 10.

CONCLUSIONS

There are many situations in which the moving contact line plays a significant, if not dominating, role; some examples of which are rivulet and coating flows, dry patch formation, and the damping of surface waves in a closed basin. An analysis of each of these problems has been inhibited by an inability to deal with the moving contact line.

For a long time, surface chemists have been satisfied with using the static contact angle as the criterion for the wettability of a solid (a static contact angle close to 0°, as measured from the liquid side of the contact line, indicates that the liquid wets the solid). From a practical point of view, this is incomplete because it does not indicate the length of time needed for the liquid to spread over the surface of the solid.

In recent years, significant advances have been made. It has been shown that the measured dynamic contact angle is probably not the actual contact angle because of the influence of the viscous forces on the shape of the meniscus in the immediate vicinity of the moving contact line. This is true even for small values of $U\mu/\sigma$. Insofar as the apparent contact angle is affected by the motion of the fluids, its value also depends on the geometry in which it is measured.

More experiments are needed to determine the reproducibility of dynamic contact-angle measurements, and also to identify the physical properties of the system to which it is sensitive. More analyses are needed with less restrictive assumptions on the capillary and Reynolds numbers.

We are closely approaching the moment when flow fields containing moving contact lines are well-posed mathematical problems.

ACKNOWLEDGMENTS

I am grateful for the insight my colleagues Eduardo Glandt, Fred Kafka, and Clifton Ngan have given me. I am also grateful for the support received from the National Science Foundation under Grant ENG77-10167.

Literature Cited

Ablett, R. 1923. An investigation of the angle of contact between paraffin wax and water. *Philos. Mag.* 46:244–56

Barker, J. A., Henderson, D. 1976. What is "liquid?" Understanding the states of matter. *Rev. Mod. Phys.* 48:587–671

Bascom, W. D., Cottington, R. L., Singleterry, C. R. 1964. Dynamic surface phenomena in the spontaneous spreading of oils on solids. In *Contact Angle, Wettability and Adhesion*, pp. 355–79. Adv. in Chem. no. 43. Washington, D.C.: Amer. Chem. Soc. 389 pp.

Berry, M. V. 1974. Simple fluids near rigid solids: statistical mechanics of density and contact angle. *J. Phys. A: Math. Nucl. Gen.* 7:231–45

Blake, T. D. 1968. The contact angle and two-phase flow. PhD thesis. Univ. Bristol, Great Britain

Blake, T. D., Haynes, J. M. 1969. Kinetics of liquid/liquid displacement. *J. Colloid Interface Sci.* 30:421–23

Buckmaster, J. 1977. Viscous sheets advancing over dry beds. *J. Fluid Mech.* 81: 735–56

Burley, R., Kennedy, B. S. 1976a. A study of the dynamic wetting behavior of polyester tapes. *Br. Polym. J.* 8:140–43

Burley, R., Kennedy, B. S. 1976b. An experimental study of air entrainment at a solid/liquid/gas interface. *Chem. Eng. Sci.* 31:901–11

Chapela, G. A., Saville, G., Thompson, S. M., Rowlinson, J. S. 1977. Computer simulation of a gas-liquid surface. *J. Chem. Soc. Faraday Trans. II.* 73:1133–44

Concus, P. 1968. Static menisci in a vertical right circular cylinder. *J. Fluid Mech.* 34:481–95

del Cerro, M. C. G., Jameson, G. 1976. Intermolecular forces and the three-phase contact line. In *Wetting, Spreading and Adhesion*, ed. J. F. Padday, pp. 61–82. London: Academic. 498 pp.

Dussan V., E. B. 1976a. On the difference between a bounding surface and a material surface. *J. Fluid Mech.* 75:609–23

Dussan V., E. B. 1976b. The moving contact line: the slip boundary condition. *J. Fluid Mech.* 77:665–84

Dussan V., E. B. 1977. Immiscible liquid displacement in a capillary tube: The moving contact line. *AIChE J.* 23:131–33

Dussan V., E. B., Davis, S. H. 1974. On the motion of a fluid-fluid interface along a solid surface. *J. Fluid Mech.* 65:71–95

Elliot, G. E. P., Riddiford, A. C. 1967.

Dynamic contact angles. I. The effect of impressed motion. *J. Colloid Interface Sci.* 23:389–98

Gauss, K. F. 1829. Principia generalia theoriae figurae fluidorum in statu aequilibrii. *Gött. Gelehrte Anz.* 1829:1641–48 = *Werke*, 5:287–92. Göttingen: K. Ges. Wiss. Gött., 1867; Hildesheim: Olms, 1973

Gibbs, J. W. 1906. *The Scientific Papers of J. Willard Gibbs, Vol. I, Thermodynamics.* New York: Longmans, Green 1906, 1931; Dover, 1961. 434 pp.

Glandt, E. D., Myers, A. L., Fitts, D. D. 1978. Physical adsorption of gases on graphitized carbon black. *Chem. Eng. Sci.* In press

Hansen, R. J., Toong, T. Y. 1971. Dynamic contact angle and its relationship to forces of Hydrodynamic origin. *J. Colloid Interface Sci.* 37:196–207

Hardy, W. B., 1919. The spreading of fluids on glass. *Philos. Mag.* 38:49–55

Hocking, L. M. 1976. A moving fluid interface on a rough surface. *J. Fluid Mech.* 76:801–17

Hocking, L. M. 1977. A moving fluid interface. Part 2. The removal of the force singularity by a slip flow. *J. Fluid Mech.* 79:209–29

Hoffman, R. 1975. A study of the advancing interface. I. Interface shape in liquid-gas systems. *J. Colloid Interface Sci.* 50:228–41

Huh, C., Mason, S. G. 1977. Effects of surface roughness on wetting (theoretical). *J. Colloid Interface Sci.* 60:11–38

Huh, C., Scriven, L. E. 1971. Hydrodynamic model of steady movement of a solid/liquid/fluid contact line. *J. Colloid Interface Sci.* 35:85–101

Inverarity, G. 1969. Dynamic wetting of glass fibre and polymer fibre. *Br. Polym. J.* 1:245–51

Irving, J. H., Kirkwood, J. G. 1950. The statistical mechanical theory of transport processes. IV. Equations of hydrodynamics. *J. Chem. Phys.* 18:817–29

Jameson, G., del Cerro, M. C. G. 1976. Theory for the equilibrium contact angle between a gas, a liquid and a solid. *J. Chem. Soc. Faraday Trans. I.* 72:883–95

Johnson, R. E., Dettre, R. H. 1964. Contact angle hysteresis. I. Study of an idealized rough surface. See Bascom et al 1964, pp. 112–35

Kafka, F. Y., Dussan V., E. B. 1978. Interpretation of dynamic contact angles in capillaries. Submitted for review.

Kirkwood, J. G., Buff, F. P. 1949. The statistical mechanical theory of surface tension. *J. Chem. Phy.* 17:338–43

Kwei, T. K., Schonhorn, H., Frisch, H. L. 1968. Kinetics of wetting of surface by polymer melts. *J. Colloid Interface Sci.* 28:543–46

Lester, G. R. 1961. Contact angles of liquids at deformable solid surfaces. *J. Colloid Sci.* 16:315–26

Lopez, J., Miller, C., Ruckenstein, E. 1976. Spreading kinetics of liquid drops. *J. Colloid Interface Sci.* 56:460–68

Miller, C. A., Ruckenstein, E. 1974. The origin of flow during wetting of solids. *J. Colloid Interface Sci.* 48:368–73

Oliver, J. F., Mason, S. G. 1977. Microspreading studies on rough surfaces by scanning electron microscopy. *J. Colloid Interface Sci.* 60:480–87

Padday, J. F. 1969. Theory of surface tension. In *Surface and Colloid Science*, ed. E. Matijević, 1:39–251. New York: Wiley. 260 pp.

Rayleigh, Lord. 1890. On the theory of surface forces. *Philos. Mag.* 30:285–98, 456–75 = *Sci. Pap.* 3:398–425. Cambridge: Univ. Press, 1902; New York: Dover, 1964

Saville, G. 1977. Computer simulation of the liquid-solid-vapor contact angle. *J. Chem. Soc. Faraday Trans. 2* 73:1122–32

Schonhorn, H., Frisch, H. L., Kwei, T. K. 1966. Kinematics of wetting of surfaces by polymer melts. *J. Appl. Phys.* 17:4967–73

Schwartz, A. M., Roder, C. A., Huey, E. 1964. Resistance to flow in capillary systems of positive contact angle. See Bascom et al 1964, pp. 250–67

Schwartz, A. M., Tejada, S. B. 1972. Studies of dynamic contact angles on solids. *J. Colloid Interface Sci.* 38:359–75

Smith, S. H. 1969. On initial value problems for the flow in a thin sheet of viscous liquid. *Z. Angew. Math. Mech.* 20:556–60

Washburn, E. W. 1921. The dynamics of capillary flow. *Phys. Rev.* 17:273–83

West, G. D. 1912. On resistance to the motion of a thread of mercury in a glass tube. *Proc. R. Soc. London Ser. A* 86:20–25

Wilson, S. D. R. 1975. A note on the measurement of dynamic contact angles. *J. Colloid Interface Sci.* 51:532–34

Yarnold, G. D. 1938. The motion of a mercury index in a capillary tube. *Proc. Phys. Soc. London* 50:540–52

Young, T. 1805. An essay on the cohesion of fluids. *Philos. Trans. R. Soc. London* 95:65–87

Zisman, W. A. 1964. Relation of equilibrium contact angle to liquid and solid constitution. See Bascom et al 1964, pp. 1–51